LBL-20946
UC-28

Lawrence Berkeley Laboratory
UNIVERSITY OF CALIFORNIA

Accelerator & Fusion
Research Division

NC515: A NEW DIPOLE CROSS-SECTION FOR SSC

S. Caspi, M. Helm, L.J. Laslett, and C. Taylor

January 1986

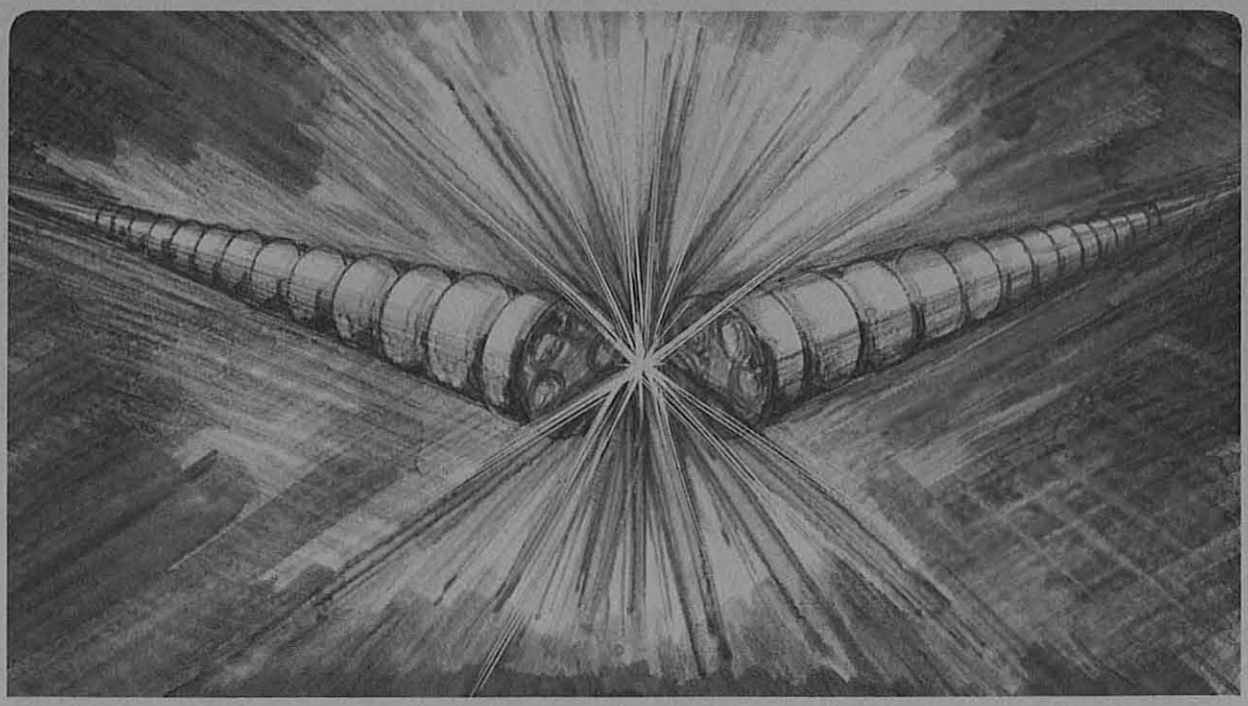

Prepared for the U.S. Department of Energy under Contract DE-AC03-76SF00098

Printed in the United States of America
Available from
National Technical Information Service
U.S. Department of Commerce
5285 Port Royal Road
Springfield, VA 22161
Price Code: A03

LBL-20946
SSC-MAG-64

NC515 - A NEW DIPOLE CROSS-SECTION FOR SSC*

S. Caspi, M. Helm, L.J. Laslett, and C. Taylor

Lawrence Berkeley Laboratory
University of California
Berkeley, CA 94720

January 1986

*This was supported by the Director, Office of Energy Research, Office of High Energy and Nuclear Physics, High Energy Physics Division, U.S. Dept. of Energy, under Contract No. DE-AC03-76SF00098.

NC515 - A NEW DIPOLE CROSS-SECTION FOR SSC

S. Caspi, M. Helm, L.J. Laslett, and C. Taylor

ABSTRACT

A new dipole cross-section for SSC is outlined which has multipole coefficients of less than 1.0×10^{-6} of the dipole field (or 0.01 units) at 1.0 cm. This cross-section has four conductor blocks (three wedges, sixteen turns) in the inner layer and two conductor blocks (one wedge, twenty turns) in the outer layer. The two layers were formed from the same types of "partially-keystoned" cable used in model magnets at LBL and BNL. Based on present cable design an operating field of 6.6 T at 4.35 K is chosen. The new cross-section "NC515" and multipoles (for μ-infinite in iron) are shown below (Figs. 1,1a).

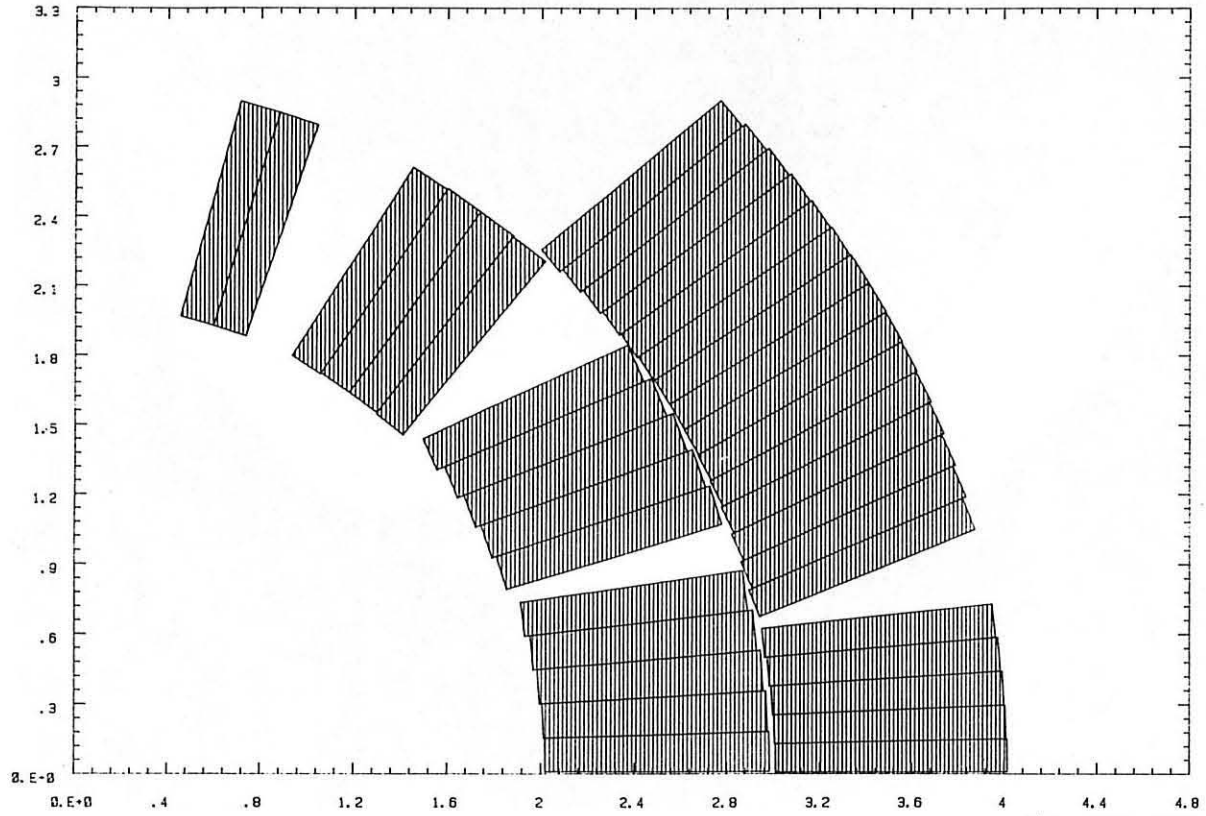

XBL 862-425

Fig. 1. A quadrant cross-section of NC515, a 4 wedge solution.

N	0	2	4	6	8	10
b_n	1.0	-1.8×10^{-8}	-8.5×10^{-8}	-4.9×10^{-7}	-1.4×10^{-7}	1.1×10^{-6}

Multipole coefficients evaluated at 1.0 cm.

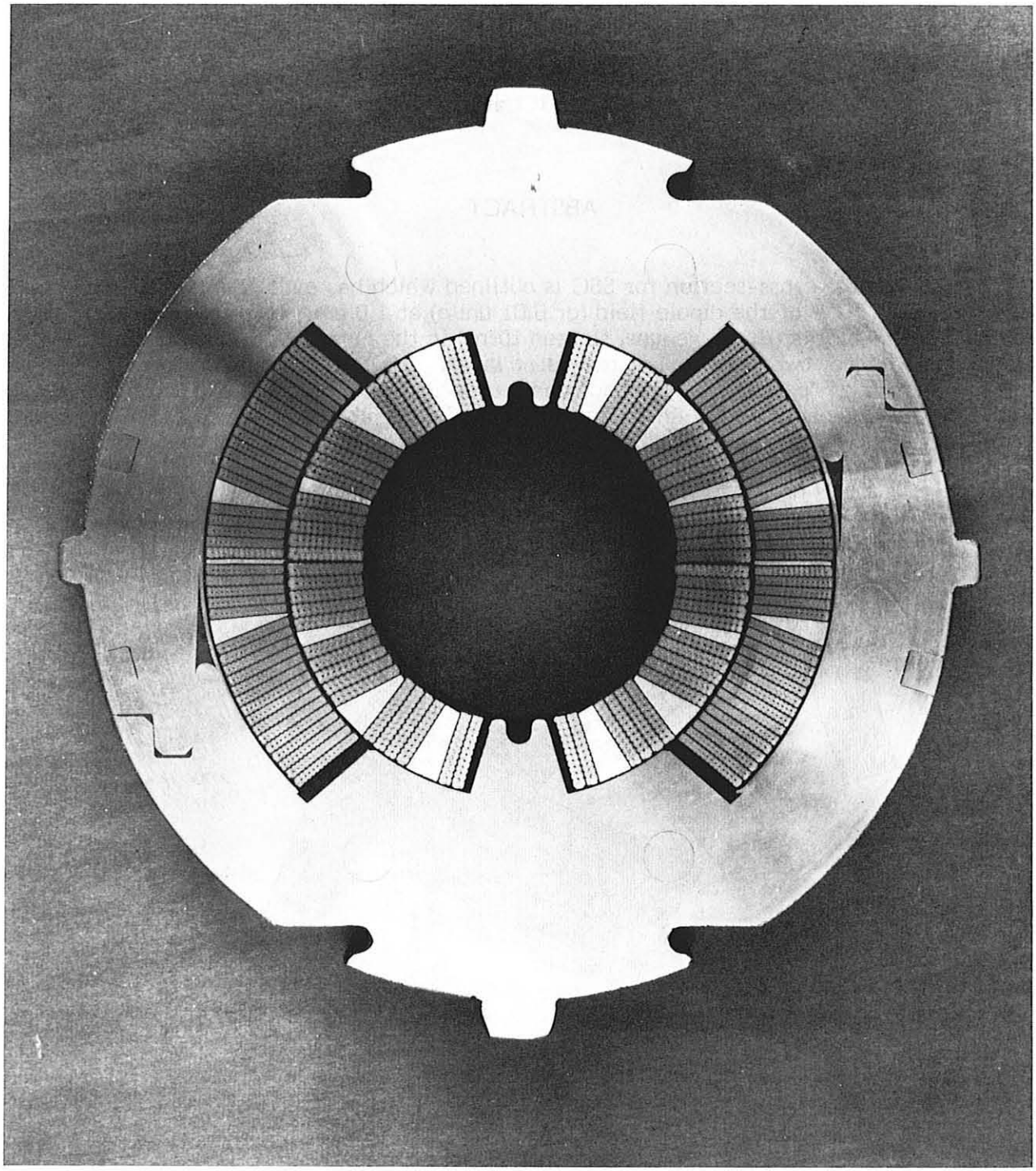

CBB 861-379

Fig. 1a. A model cross-section of NC515.

MAGNET DESIGN

Discussions with the SSC Central Design Group suggested that we attempt to redesign dipole magnet C5 so that higher multipoles -- b_8 (18-pole) and above -- are less than 0.2 units of the dipole field at a radius of 1.0 cm. Also we have increased the midplane insulation thickness from 4 mil, used in current model magnets, to 8 mil (not including conductor insulation). In this new design model magnets can be constructed with the available collars, which was a desired but not necessary consideration. Also, the wedge shape is constrained to stay above a minimum practical size at its "pointed" end to permit precise positioning and to avoid sharp edges. The character of this new design and steps taken to develop it are outlined in the remainder of this report.

The BNL program PARTIALKEYSTONE was available to search for "good" (low multipole value) cross-sections. We modified PARTIALKEYSTONE so that current blocks may deviate from a purely radial orientation. We also developed independent techniques for providing PARTIALKEYSTONE with preliminary cross-sections for optimization. We realized that there are many solutions that are "good" but differ very much in their geometry, and that at which one of these "good" solutions PARTIALKEYSTONE arrives depends on where it starts out. We therefore used some assumptions to choose starting points likely to result in "good" designs. For further information see the appendices.

Using the modified PARTIALKEYSTONE we examined several families of three-wedge cross-sections (Fig 2). For mechanical and magnetic considerations an additional wedge was introduced into the inner layer of a particularly promising cross-section (four wedges in all). Optimization of this four-wedge case yielded a solution with a better field quality than had been found in any of the three-wedge cases. By restricting the number of turns in the outer layer of this case to twenty, and moving the position of the outer-layer wedge, a cross-section with low multipole values and acceptable pole angles was found. This design is NC515 (Fig. 1).

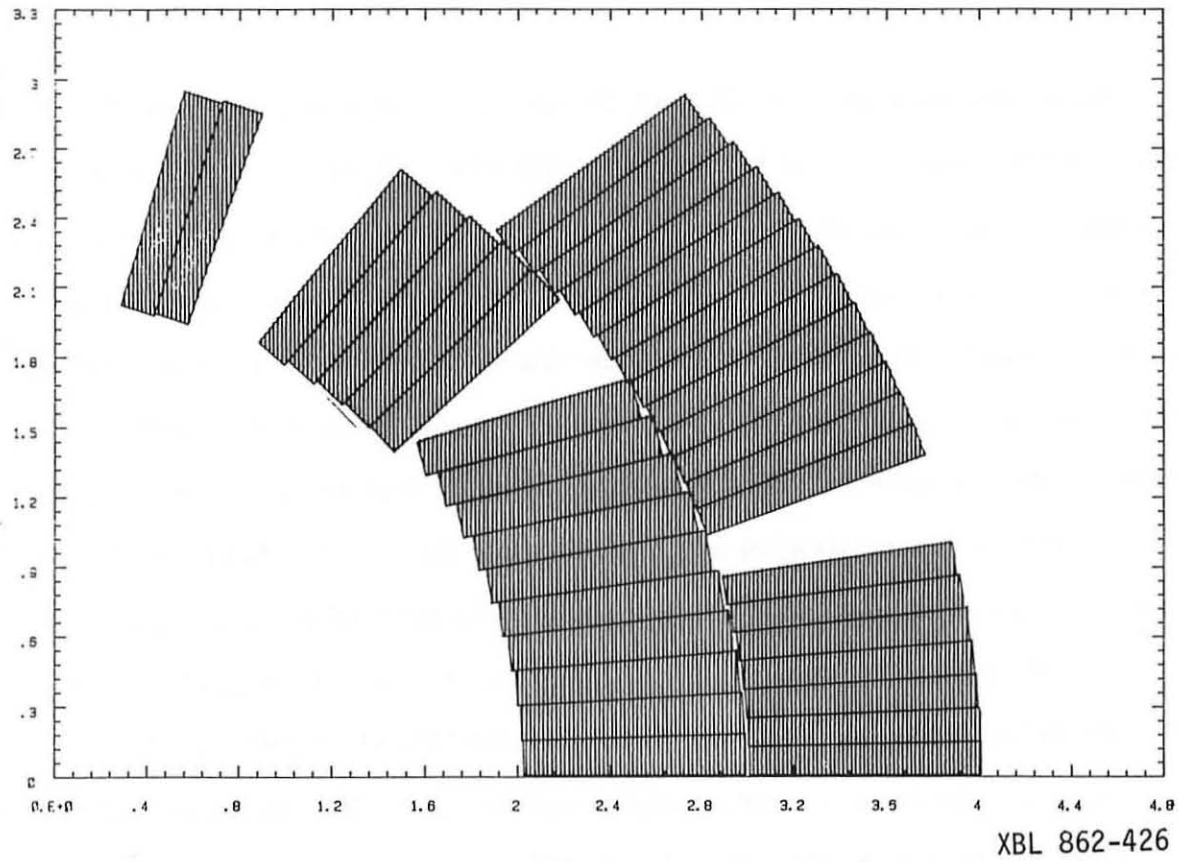

Fig. 2. A quadrant cross-section of "TP 3", a 3 wedge solution. The following multipoles have been calculated for "TP 3".

N	0	2	4	6	8	10
b_n	1.0	1.14×10^{-7}	6.87×10^{-7}	1.15×10^{-5}	6.6×10^{-6}	-1.2×10^{-5}

We used the computer programs POISSON to study the effect iron saturation and current distribution have on the harmonic content of NC515, refinements not available in PARTIALKEYSTONE.

Several POISSON runs were made using a cross-section very closely approximating NC515 (in POISSON, it is difficult to model individual turns inside conductor blocks). We modelled two different current distributions. In the Constant Density model, each block of conductor is assumed to have a constant current density

(the same assumption used by PARTIALKEYSTONE). A better approximation to the distribution of current in the conductor is the Split Density model, where each layer of conductor is divided radially in half, and each half assigned half the total current; the number of strands is assumed to be equal in each half, while the effective cross-sectional area per strand differs radially due to keystoning. The difference between these two models is shown in Table 1.

Table 1 - Difference in multipoles between Split Density and Constant Density models (at 1 cm)

(10^{-4} dipole units)

multipoles	b_2	b_4	b_6	b_8
b_n(S.D.)-b_n(C.D.)	-3.76	-0.75	-0.145	-0.011

Since we felt the Split Density model to be more accurate than the Constant Density model, we designed a slightly revised cross-section geometry to compensate for the multipole differences between them. We asked PARTIALKEYSTONE to optimize the wedge dimensions to arrive at a solution where the first four multipoles are the inverse of those in Table 1. This revised cross-section geometry--NC515AUG--should result in a magnet with very low multipoles. Included in Appendix A are the PARTIALKEYSTONE input and output for both - NC515 - and - NC515AUG.

OPERATING FIELD

It is difficult to predict precisely the critical current of a magnet since the conditions under which a cable in the magnet "quenches" cannot be duplicated in tests of short sections of cable. However, observation of critical current achieved in Design D model magnets at BNL and LBL constructed of cable with varying strand current

density indicates that an operating current density, J_0 of 80% of the uncabled strand current density J_c, is a reasonable design value. This allows for some degradation during cabling and some operating margin. J_c is determined at the maximum field value calculated at the edge of the cable and at the maximum operating temperature of 4.35K provided by the helium coolant.

Cable properties are described in Table 2.

Table 2

	Inner	Outer
Strand Diameter	.0318 in.	.0255 in.
Number of Strands	23	30
Copper to Superconductor Ratio	1.3	1.8
Cable dimensions (including insulation) used in the calculation		
Cable Width	.9627 cm.	1.0058 cm.
Cable Thickness (nominal)	.063189 in.	.052953 in.
Cable Keystone	.0107 in.	.0083 in.

In addition to these mechanical specifications, the minimum critical current of the strands is characterized by J_c of 2750 A/mm^2 at 4.22K, 5T, and $\rho = 10^{-14}\Omega$-m. Scaling of J_c with temperature and field is done using the following relationship.

$$J_c(T,B) = P_1 \left(1 - \frac{T - 4.2}{P_2 - P_3 B}\right)\left(1 + P_4 B\right)$$

where

$$P_1 = 5509.72 \frac{J_c(4.22K,\ 5T)}{2750} \qquad (1)$$

[$J_c(4.22K, 5T) = 2750$ A/mm^2 for this design, as cited above]

$$P_2 = 7.81042$$

$$P_3 = 0.778448$$

$$P_4 = -.996643$$

Table 3 gives the operating conditions for the magnet at 4.35K and at 4.50 K for equivalent operating margin, J_c/J_o. (Current density, J is in A/mm^2.)

Table 3

			Inner Coil				Outer Coil			
T(K)	B_o(T)	I(A)	B_{max}	J_o	J_c	J_c/J_o	B_{max}	J_o	J_c	J_c/J_o
4.35	6.595	6485	6.961	1265	1581	1.250	5.566	1837	2347	1.278
4.50	6.466	6357	6.825	1241	1550	1.250	5.457	1801	2301	1.278

Table 3 shows that the inner and outer cables are reasonably well balanced with the inner coil having slightly less operating margin than the outer coil; however, this small difference is not significant compared with other variations in cable behavior that affect maximum operating field. Therefore, at 4.35T, the operating field is chosen to be 6.6T for cross section NC515; other cross sections would result in variations from this depending on details of magnetic field in the windings.

(1)This linear relationship is accurate within the range of this design (M. McAshan, personal communication).

EFFECT OF REAL IRON

We have calculated the effect of iron saturation on the multipoles for various field levels and, also, the effect of iron stacking factors of 1.0 and 0.97. These calculations used the NC515 cross-section , and iron with 11.14 cm ID, 26.66 cm OD and no holes. A tabulation of these results for the first four multipoles is given in Table 4, and a plot of sextupole versus field level (including stacking factor = 1.0 and 0.97) is given in Fig. 3.

Included in Fig. 4 are the geometry and flux plot for NC515 solved by POISSON. Note that each layer was split in half as an approximation to the radial current distribution due to keystoning.

Table 4 assumes that a perfect dipole exists at low field (with real iron)-- i.e. all multipole coefficients become equal to zero at B_0 = -0.6597 T. The values in Table 4 accordingly have been normalized by subtracting the multipoles for the high field cases from the corresponding values in the low field (perfect dipole) case. In Table 5 are shown the values and locations of the maximum field in each layer for a case where B_0 = 6.5 T, with transfer functions and stored energy in Table 6. Note that this energy is for the full cross-section, per unit length. The coil inductance at 6400 A is computed to be 3.146 mHy/m.

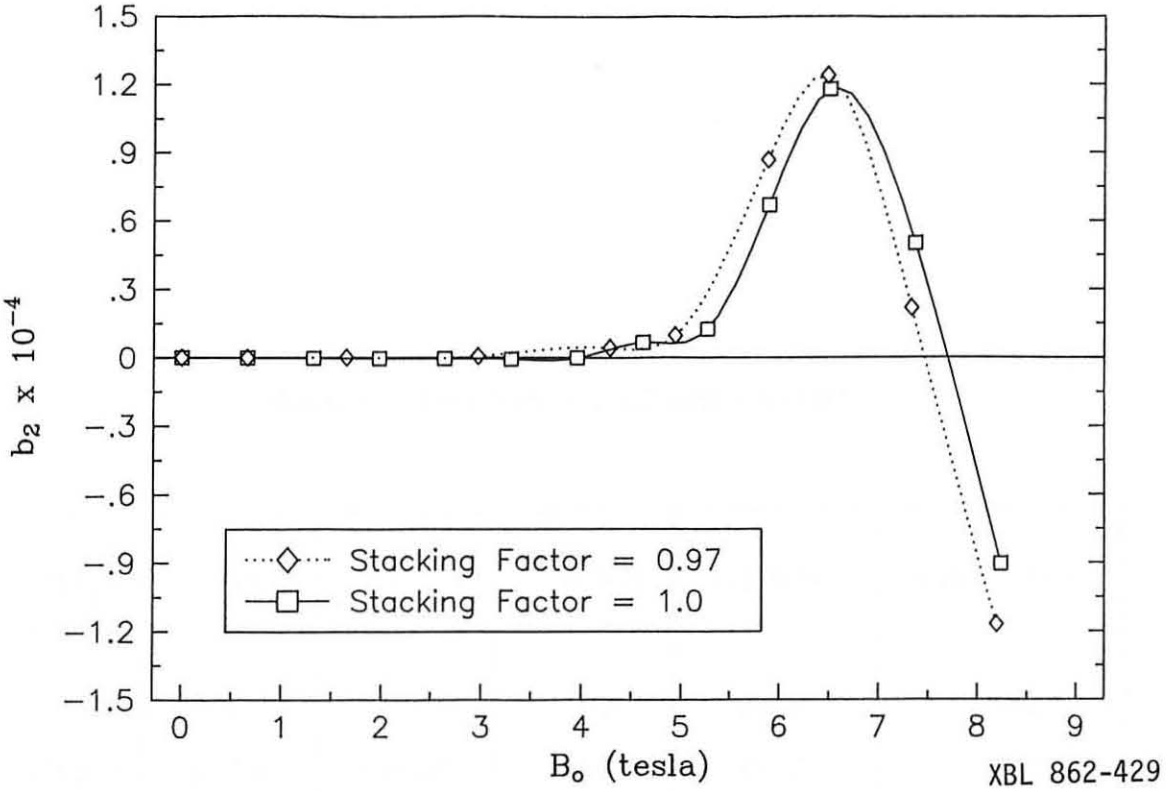

Fig. 3. Sextupole as a function of the dipole field for real iron, 10.5" O.D..

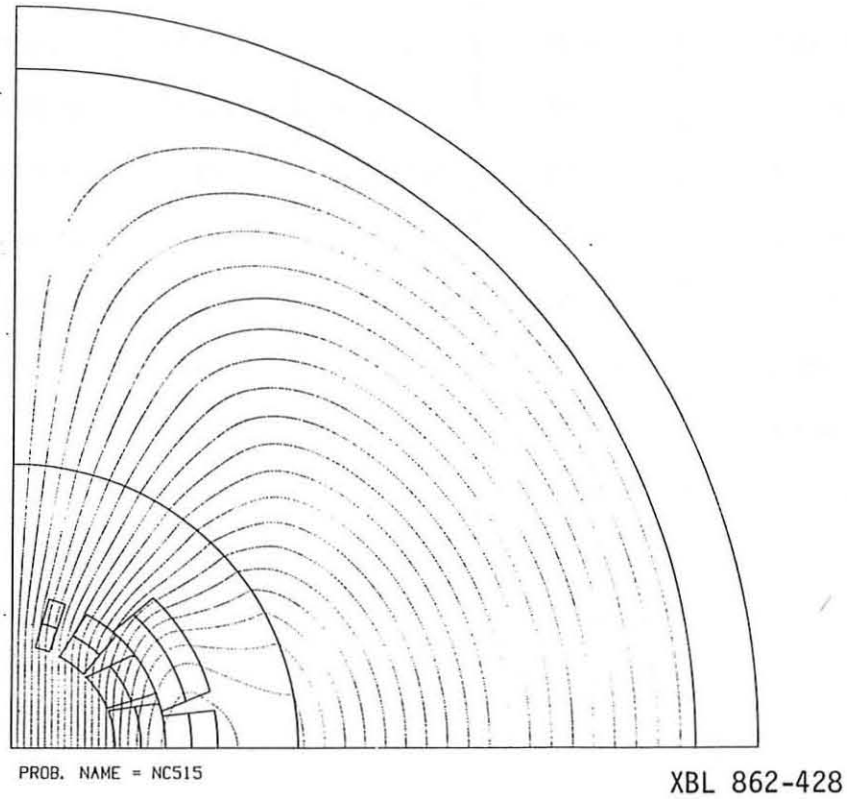

Fig. 4. Flux plot of NC515 solved by POISSON. Inner coil radius 20.193 mm, outer coil radius 40.132 mm, iron inner radius 55.70 mm, iron outer radius 133.30 mm.

Table 4 - Iron Saturation Effects on Multipoles

CURRENT (A)	FIELD (T)	$b_2 \times 10^{-4}$	$b_4 \times 10^{-4}$	$b_6 \times 10^{-4}$	$b_8 \times 10^{-4}$
640.0	-0.66	0.0	0.0	0.0	0.0
1280.0	-1.32	-0.0005	-0.0089	-0.0089	0.0171
1920.0	-1.98	-0.0017	-0.0090	-0.0089	0.0172
2560.0	-2.64	-0.0043	-0.0090	-0.0089	0.0172
3200.0	-3.30	-0.0074	-0.0090	-0.0089	0.0172
3840.0	-3.96	-0.0007	-0.0094	-0.0089	0.0172
4480.0	-4.62	0.0666	-0.0109	-0.0089	0.0172
5120.0	-5.27	0.1251	-0.019	-0.0095	0.0172
5760.0	-5.90	0.669	-0.035	-0.010	0.0180
6400.0	-6.51	1.1793	-0.0512	-0.0137	0.0168
7360.0	-7.37	0.5008	-0.0837	-0.0149	0.0199
8384.0	-8.24	-0.905	-0.1203	-0.0189	0.0209

Table 5 - Peak Field Locations

(B_0 = 6.5 T)

μ	Layer	X(cm)	Y(cm)	B_{max}/B_o
infinite	inner	0.44	2.02	1.0497
	outer	2.20	2.50	0.842
real iron	inner	0.45	2.15	1.0555
	outer	2.15	2.45	0.844

Table 6 - Transfer Function and Stored Energy

B_o (T)	Transfer function (G/A)	Stored Energy (KJ/m)
μ = ∞ (6400A)	10.316	-
1.32	10.309	2.62
6.5 (6400A)	10.172	64.42

APPENDIX A

PARTIALKEYSTONE

The computer program PARTIALKEYSTONE was the primary tool used in developing the new cross-section. (This program was first written by R. Fernow and G. Morgan at BNL and is known there, perhaps, as MAG2PL). Based on preliminary use of this program we felt some changes were needed in the program and the method of using it, which would make the search for a new cross-section easier and more effective. We summarize these changes below.

Originally PARTIALKEYSTONE would radially-align conductor blocks. By this we mean that the angular center between the starting and ending sides of a block (or clockwise and counter-clockwise faces of a block) would lie along a radial line to the origin. While perhaps desirable from mechanical considerations this condition unnecessarily constrains the problem in that it may exclude many usable solutions--perhaps those satisfying our stringent multipole coefficient requirements. We accordingly introduced the ability to "twist" a block. The conductor block is twisted by changing the angle between the faces of the preceding wedge.

We realized that some techniques used by the optimizer in PARTIALKEYSTONE, such as Monte Carlo searches, were very time-consuming and not very helpful in finding the quality of cross-section we needed. It was also not very helpful or even mathematically sound to optimize the number of conductor turns -- a discrete quantity -- with an algorithm which treats the number of turns as a continuous variable. Therefore we developed techniques for finding good starting geometries for conductor layout. The starting geometry provides PARTIALKEYSTONE with a complete account of the conductor in a cross-section: the number of blocks in each layer, and the number of turns in each block. PARTIALKEYSTONE can then optimize the shape of the wedges. A starting geometry is based on a thin two-layer multi-block design with

infinite permeability in iron. This is discussed in detail in Appendix B. The starting geometry can be quickly translated to real dimensions for PARTIALKEYSTONE using a LOTUS 1-2-3 worksheet. The worksheet can translate many different starting geometries at once, and permits the rapid substitution of different cable dimensions, saving a lot of laborious calculation.

It was thought that using a fully-keystoned conductor with the same midwidth as the partially-keystoned conductor would be helpful in searching for good solutions with PARTIALKEYSTONE. A partially-keystoned geometry was constructed based on the geometry of a good fully-keystoned cross-section. Then the wedges were optimized (changed in width and "twist") to restore a good solution.

These techniques were used to find a new three-wedge cross-section (Fig. 2). This cross-section was acceptable magnetically, but required some mechanical improvement. The fourth wedge was then introduced into block one of layer one, and the cross-section re-optimized to produce NC515 (Fig. 1). The block angles and wedge spacing of the three-wedge solution were used as the starting geometry, rather than the techniques described above. The "twists" of blocks in both layers were tuned to provide the lowest multipole coefficient values possible.

These new techniques were helpful, in general, in arriving at cross-section NC515. The starting geometry technique provided good preliminary cross-sections. It also showed us that good cross-sections fell into several distinct families, and a particularly good family was discovered right away. Unfortunately the computer program implementing this technique was limited to three wedge solutions. "Twist" of the block enabled us to design reasonably shaped and sized wedges, keep pole angles within bounds, and introduced an additional variable for optimization of multipoles (mostly sextupole and decapole). The latter was also its weakness: the "twist" optimization could not be introduced into PARTIALKEYSTONE's optimization data structure. Using fully-keystoned solutions was also not without benefit either, in part

as a motivation for the other changes, and also as a means of getting starting wedge angles for partially-keystoned solutions.

We conclude from the above that it would be helpful to integrate techniques for picking starting points with PARTIALKEYSTONE, and including the "twist" or wedge angle in PARTIALKEYSTONE's optimization. It might also be helpful to develop an algorithm that could vary the number of conductor turns and blocks discretely.

Table 7 - NC515 geometry

PK OUTPUT

```
IL,IB,IC,CXY,ANG  1  1  1  2.0188   .0102    2.0168   .1571    2.9792   .1842    2.9816   .0102     .29  4.45  3.54   .20
IL,IB,IC,CXY,ANG  1  1  2  2.0109   .1569    2.0047   .3037    2.9660   .3580    2.9733   .1841    4.46  8.61  6.88  3.54
IL,IB,IC,CXY,ANG  1  1  3  1.9936   .3030    1.9832   .4496    2.9426   .5310    2.9549   .3574    8.64 12.77 10.23  6.90
IL,IB,IC,CXY,ANG  1  1  4  1.9669   .4482    1.9524   .5944    2.9090   .7029    2.9262   .5296   12.84 16.93 13.58 10.26
IL,IB,IC,CXY,ANG  1  1  5  1.9307   .5919    1.9121   .7377    2.8653   .8731    2.8874   .7004   17.05 21.10 16.95 13.64
PHIEND,RI,RO=      21.0960      2.0332      2.9820
IL,IB,WANG=   1    2   .1529E+01
IL,IB,IC,CXY,ANG  1  3  1  1.8604   .7781    1.8162   .9182    2.7301  1.2211    2.7825  1.0551   22.70 26.82 24.10 20.77
IL,IB,IC,CXY,ANG  1  3  2  1.7994   .9126    1.7512  1.0514    2.6562  1.3800    2.7133  1.2156   26.89 30.98 27.45 24.13
IL,IB,IC,CXY,ANG  1  3  3  1.7296  1.0436    1.6775  1.1809    2.5729  1.5349    2.6346  1.3722   31.11 35.14 30.82 27.51
IL,IB,IC,CXY,ANG  1  3  4  1.6510  1.1705    1.5951  1.3063    2.4801  1.6854    2.5464  1.5245   35.33 39.32 34.20 30.91
IL,IB,IC,CXY,ANG  1  3  5  1.5638  1.2929    1.5040  1.4271    2.3780  1.8311    2.4488  1.6720   39.58 43.50 37.60 34.33
PHIEND,RI,RO=      43.4969      2.0500      2.9820
IL,IB,WANG=   1    4   .2178E+01
IL,IB,IC,CXY,ANG  1  5  1  1.4159  1.4510    1.3005  1.5419    1.8855  2.3065    2.0223  2.1988   45.70 49.86 50.74 47.39
IL,IB,IC,CXY,ANG  1  5  2  1.3039  1.5464    1.1859  1.6340    1.7492  2.4148    1.8889  2.3110   49.86 54.03 54.08 50.74
IL,IB,IC,CXY,ANG  1  5  3  1.1861  1.6343    1.0658  1.7185    1.6068  2.5149    1.7494  2.4151   54.03 58.19 57.43 54.08
IL,IB,IC,CXY,ANG  1  5  4  1.0630  1.7145     .9404  1.7953    1.4587  2.6067    1.6040  2.5109   58.20 62.35 60.77 57.43
PHIEND,RI,RO=      62.3547      2.0206      2.9820
IL,IB,WANG=   1    6   .6530E+01
IL,IB,IC,CXY,ANG  1  7  1   .7282  1.8866     .5884  1.9317     .8712  2.8520    1.0369  2.7985   68.89 73.06 73.01 69.67
IL,IB,IC,CXY,ANG  1  7  2   .5883  1.9314     .4472  1.9726     .7040  2.9005     .8711  2.8517   73.06 77.23 76.36 73.01
PHIEND,RI,RO=      77.2252      2.0195      2.9820
IL,IB,IC,CXY,ANG  2  1  1  3.0072   .0102    3.0059   .1341    4.0115   .1552    4.0130   .0102     .19  2.55  2.22   .15
IL,IB,IC,CXY,ANG  2  1  2  3.0030   .1341    2.9991   .2579    4.0040   .3001    4.0086   .1551    2.56  4.92  4.29  2.22
IL,IB,IC,CXY,ANG  2  1  3  2.9936   .2577    2.9871   .3815    3.9910   .4447    3.9986   .2999    4.92  7.28  6.36  4.29
IL,IB,IC,CXY,ANG  2  1  4  2.9792   .3810    2.9701   .5046    3.9724   .5889    3.9830   .4442    7.29  9.64  8.43  6.36
IL,IB,IC,CXY,ANG  2  1  5  2.9596   .5038    2.9479   .6272    3.9483   .7324    3.9619   .5880    9.66 12.01 10.51  8.44
PHIEND,RI,RO=      12.0105      3.0074      4.0098
IL,IB,WANG=   2    2   .1740E+01
IL,IB,IC,CXY,ANG  2  3  1  2.9304   .7171    2.8817   .8311    3.8028  1.2354    3.8597  1.1020   13.75 16.09 18.00 15.93
IL,IB,IC,CXY,ANG  2  3  2  2.8969   .8378    2.8459   .9507    3.7582  1.3742    3.8179  1.2420   16.13 18.47 20.09 18.02
IL,IB,IC,CXY,ANG  2  3  3  2.8585   .9566    2.8051  1.0685    3.7084  1.5110    3.7709  1.3801   18.50 20.85 22.17 20.10
IL,IB,IC,CXY,ANG  2  3  4  2.8153  1.0735    2.7596  1.1842    3.6535  1.6456    3.7186  1.5160   20.87 23.23 24.25 22.18
IL,IB,IC,CXY,ANG  2  3  5  2.7675  1.1883    2.7095  1.2978    3.5934  1.7778    3.6613  1.6496   23.24 25.59 26.32 24.25
IL,IB,IC,CXY,ANG  2  3  6  2.7150  1.3008    2.6547  1.4091    3.5284  1.9075    3.5990  1.7808   25.60 27.96 28.40 26.33
IL,IB,IC,CXY,ANG  2  3  7  2.6580  1.4110    2.5954  1.5180    3.4585  2.0346    3.5317  1.9094   27.96 30.32 30.47 28.40
IL,IB,IC,CXY,ANG  2  3  8  2.5965  1.5187    2.5317  1.6244    3.3838  2.1589    3.4596  2.0353   30.32 32.68 32.54 30.47
IL,IB,IC,CXY,ANG  2  3  9  2.5307  1.6237    2.4637  1.7280    3.3044  2.2803    3.3827  2.1583   32.68 35.05 34.61 32.54
IL,IB,IC,CXY,ANG  2  3 10  2.4606  1.7259    2.3914  1.8288    3.2203  2.3986    3.3012  2.2782   35.05 37.41 36.68 34.61
IL,IB,IC,CXY,ANG  2  3 11  2.3862  1.8253    2.3149  1.9267    3.1317  2.5137    3.2151  2.3951   37.41 39.77 38.75 36.68
IL,IB,IC,CXY,ANG  2  3 12  2.3078  1.9215    2.2344  2.0214    3.0387  2.6255    3.1245  2.5086   39.78 42.14 40.83 38.76
IL,IB,IC,CXY,ANG  2  3 13  2.2253  2.0146    2.1498  2.1129    2.9413  2.7337    3.0296  2.6186   42.15 44.50 42.91 40.84
IL,IB,IC,CXY,ANG  2  3 14  2.1389  2.1043    2.0613  2.2011    2.8396  2.8383    2.9303  2.7251   44.53 46.88 44.99 42.92
IL,IB,IC,CXY,ANG  2  3 15  2.0486  2.1906    1.9690  2.2857    2.7338  2.9391    2.8268  2.8278   46.92 49.26 47.07 45.01
PHIEND,RI,RO=      49.2562      3.0074      4.0055
```

```
 K     PHIST      TURNS      RIN       ROUT       I/L      THICK     PHIEND
 1    4.0000     7.0000    2.0193    2.9820    1.0000   63.1890   10.7000    0.0000
 2    4.0000     3.0000    3.0074    4.0132    1.0000   52.9530    8.3000    0.0000
```

PK INPUT

```
      1 N1        .5000E+01 .1000E+01 .1000E+01 .1200E+02
      2 W2        .1528E+01 .5        .7200E+00 .1200E+02
      3 N3        .5000E+01 .1000E+01 .1000E+01 .1000E+02
      4 W4        .2178E+01 .5        .3500E+00 .1200E+02
      5 N5        .4000E+01 .1000E+01 .3000E+01 .7000E+01
      6 W6        .6530E+01 .5        .3500E+00 .1200E+02
      7 N7        .2000E+01 .1000E+01 .1000E+01 .4000E+01
     11 N11       .5000E+01 .2000E+01 .5000E+01 .9000E+01
     12 W12       .1741E+01 .5        .7200E+00 .1200E+02
     13 N13       .1500E+02 .1000E+01 .1200E+02 .1600E+02

$FCNIN RFE=5.5702,ROPT=1.00$
   1    4
2         0.0        1.
4         0.0        1.
6         0.0        1.
8         0.0        1.
   2
1  4.0    7.         2.0193       2.9820    1.         63.189    10.7
2  4.0    3.         3.0074       4.0132    1.         52.953     8.3
 $TWIST pb(5) = 26.15326 pb(3) = 8.6332   pb(7)=13.8672 $
FIX                 1
FIX                 3
FIX                 5
FIX                 7
FIX                11
FIX                13
CALL FCN            3
SIMPLEX
CALL FCN            3
PUNCH
EXIT
END
```

Table 8 - NC515AUG geometry

PK OUTPUT

```
IL,IB,IC,CXY,ANG  1  1  1  2.0188   .0102   2.0168   .1571   2.9792   .1842   2.9816   .0102    .29  4.45  3.54   .20
IL,IB,IC,CXY,ANG  1  1  2  2.0109   .1569   2.0047   .3037   2.9660   .3580   2.9733   .1841   4.46  8.61  6.88  3.54
IL,IB,IC,CXY,ANG  1  1  3  1.9936   .3030   1.9832   .4496   2.9426   .5310   2.9549   .3574   8.64 12.77 10.23  6.90
IL,IB,IC,CXY,ANG  1  1  4  1.9669   .4482   1.9524   .5944   2.9090   .7029   2.9262   .5296  12.84 16.93 13.58 10.26
IL,IB,IC,CXY,ANG  1  1  5  1.9307   .5919   1.9121   .7377   2.8653   .8731   2.8874   .7004  17.05 21.10 16.95 13.64
PHIEND,RI,RO=      21.0960      2.0332      2.9820
IL,IB,WANG=   1   2   .1988E+01
IL,IB,IC,CXY,ANG  1  3  1  1.8541   .7932   1.8099   .9333   2.7238  1.2362   2.7762  1.0702  23.16 27.28 24.41 21.08
IL,IB,IC,CXY,ANG  1  3  2  1.7922   .9275   1.7440  1.0662   2.6490  1.3948   2.7061  1.2304  27.36 31.44 27.77 24.45
IL,IB,IC,CXY,ANG  1  3  3  1.7215  1.0580   1.6694  1.1954   2.5648  1.5494   2.6265  1.3866  31.58 35.61 31.14 27.83
IL,IB,IC,CXY,ANG  1  3  4  1.6420  1.1846   1.5860  1.3204   2.4710  1.6995   2.5373  1.5386  35.81 39.78 34.52 31.23
IL,IB,IC,CXY,ANG  1  3  5  1.5538  1.3066   1.4940  1.4408   2.3680  1.8448   2.4388  1.6857  40.06 43.96 37.92 34.65
PHIEND,RI,RO=      43.9612      2.0517      2.9820
IL,IB,WANG=   1   4   .1999E+01
IL,IB,IC,CXY,ANG  1  5  1  1.4082  1.4576   1.2928  1.5485   1.8779  2.3132   2.0146  2.2054  45.99 50.14 50.93 47.59
IL,IB,IC,CXY,ANG  1  5  2  1.2959  1.5525   1.1779  1.6401   1.7412  2.4210   1.8809  2.3171  50.15 54.31 54.28 50.93
IL,IB,IC,CXY,ANG  1  5  3  1.1778  1.6399   1.0574  1.7242   1.5984  2.5206   1.7411  2.4208  54.31 58.48 57.62 54.28
IL,IB,IC,CXY,ANG  1  5  4  1.0544  1.7196    .9317  1.8005   1.4500  2.6118   1.5954  2.5161  58.49 62.64 60.96 57.62
PHIEND,RI,RO=      62.6398      2.0208      2.9820
IL,IB,WANG=   1   6   .6069E+01
IL,IB,IC,CXY,ANG  1  7  1   .7340  1.8846    .5942  1.9297    .8771  2.8500   1.0428  2.7965  68.72 72.88 72.89 69.55
IL,IB,IC,CXY,ANG  1  7  2   .5942  1.9298    .4532  1.9709    .7100  2.8989    .8771  2.8501  72.88 77.05 76.24 72.89
PHIEND,RI,RO=      77.0500      2.0195      2.9820
IL,IB,IC,CXY,ANG  2  1  1  3.0072   .0102   3.0059   .1341   4.0115   .1552   4.0130   .0102    .19  2.55  2.22   .15
IL,IB,IC,CXY,ANG  2  1  2  3.0030   .1341   2.9991   .2579   4.0040   .3001   4.0086   .1551   2.56  4.92  4.29  2.22
IL,IB,IC,CXY,ANG  2  1  3  2.9936   .2577   2.9871   .3815   3.9910   .4447   3.9986   .2999   4.92  7.28  6.36  4.29
IL,IB,IC,CXY,ANG  2  1  4  2.9792   .3810   2.9701   .5046   3.9724   .5889   3.9830   .4442   7.29  9.64  8.43  6.36
IL,IB,IC,CXY,ANG  2  1  5  2.9596   .5038   2.9479   .6272   3.9483   .7324   3.9619   .5880   9.66 12.01 10.51  8.44
PHIEND,RI,RO=      12.0105      3.0074      4.0098
IL,IB,WANG=   2   2   .9865E+00
IL,IB,IC,CXY,ANG  2  3  1  2.9396   .6785   2.8924   .7931   3.8187  1.1852   3.8739  1.0511  13.00 15.33 17.24 15.18
IL,IB,IC,CXY,ANG  2  3  2  2.9076   .7996   2.8581   .9132   3.7760  1.3247   3.8339  1.1917  15.38 17.72 19.33 17.27
IL,IB,IC,CXY,ANG  2  3  3  2.8708   .9189   2.8190  1.0315   3.7280  1.4621   3.7887  1.3304  17.75 20.10 21.41 19.35
IL,IB,IC,CXY,ANG  2  3  4  2.8292  1.0364   2.7750  1.1478   3.6748  1.5974   3.7383  1.4669  20.12 22.47 23.49 21.43
IL,IB,IC,CXY,ANG  2  3  5  2.7829  1.1518   2.7263  1.2621   3.6165  1.7304   3.6827  1.6013  22.48 24.84 25.57 23.50
IL,IB,IC,CXY,ANG  2  3  6  2.7319  1.2650   2.6730  1.3741   3.5532  1.8609   3.6221  1.7333  24.85 27.21 27.64 25.57
IL,IB,IC,CXY,ANG  2  3  7  2.6763  1.3759   2.6152  1.4838   3.4850  1.9889   3.5565  1.8628  27.21 29.57 29.71 27.64
IL,IB,IC,CXY,ANG  2  3  8  2.6163  1.4844   2.5529  1.5909   3.4119  2.1142   3.4861  1.9896  29.57 31.93 31.78 29.71
IL,IB,IC,CXY,ANG  2  3  9  2.5518  1.5903   2.4862  1.6954   3.3341  2.2366   3.4108  2.1136  31.93 34.29 33.86 31.79
IL,IB,IC,CXY,ANG  2  3 10  2.4830  1.6934   2.4153  1.7972   3.2516  2.3560   3.3309  2.2346  34.29 36.65 35.93 33.86
IL,IB,IC,CXY,ANG  2  3 11  2.4100  1.7937   2.3401  1.8960   3.1645  2.4723   3.2464  2.3526  36.66 39.02 38.00 35.93
IL,IB,IC,CXY,ANG  2  3 12  2.3329  1.8910   2.2608  1.9918   3.0729  2.5852   3.1573  2.4672  39.03 41.38 40.07 38.01
IL,IB,IC,CXY,ANG  2  3 13  2.2516  1.9851   2.1774  2.0844   2.9770  2.6947   3.0638  2.5785  41.40 43.75 42.15 40.08
IL,IB,IC,CXY,ANG  2  3 14  2.1664  2.0760   2.0901  2.1737   2.8767  2.8007   2.9659  2.6863  43.78 46.12 44.23 42.17
IL,IB,IC,CXY,ANG  2  3 15  2.0772  2.1634   1.9989  2.2596   2.7722  2.9028   2.8638  2.7904  46.17 48.50 46.32 44.26
PHIEND,RI,RO=      48.5024      3.0074      4.0055
```

K	PHIST	TURNS	RIN	ROUT	I/L	THICK	PHIEND	
1	4.0000	7.0000	2.0193	2.9820	1.0000	63.1890	10.7000	0.0000
2	4.0000	3.0000	3.0074	4.0132	1.0000	52.9530	8.3000	0.0000

PK INPUT

```
NC515-augmented multipoles
        1 N1        .5000E+01 .1000E+01 .1000E+01 .1200E+02
        2 W2        .1528E+01 .5        .7200E+00 .1200E+02
        3 N3        .5000E+01 .1000E+01 .1000E+01 .1000E+02
        4 W4        .2178E+01 .5        .3500E+00 .1200E+02
        5 N5        .4000E+01 .1000E+01 .3000E+01 .7000E+01
        6 W6        .6530E+01 .5        .3500E+00 .1200E+02
        7 N7        .2000E+01 .1000E+01 .1000E+01 .4000E+01
       11 N11       .5000E+01 .2000E+01 .5000E+01 .9000E+01
       12 W12       .1741E+01 .5        .7200E+00 .1200E+02
       13 N13       .1500E+02 .1000E+01 .1200E+02 .1600E+02

 $FCNIN RFE=5.5702,ROPT=1.00$
    1    4
 2         3.766      1.
 4         0.747      1.
 6         0.145      1.
 8         0.0111     1.
    2
 1  4.0    7.         2.0193       2.9820    1.         63.189    10.7
 2  4.0    3.         3.0074       4.0132    1.         52.953     8.3
 $TWIST pb(5) = 26.15326 pb(3) = 8.6332   pb(7)=13.8672 $
FIX                 1
FIX                 3
FIX                 5
FIX                 7
FIX                11
FIX                13
CALL FCN            3
SIMPLEX
CALL FCN            3
PUNCH
EXIT
END
```

APPENDIX B

Orientation Work Preparatory to Use of the Program PARTIALKEYSTONE

Introduction

The use of the Program PARTIALKEYSTONE, to provide a two-dimensional winding design for dipole magnets of acceptable harmonic content, can be facilitated by providing suitable starting points based on highly idealized winding configurations. These idealized configurations assumed the usual quadrant symmetry characteristic of dipole windings, and in a single quadrant employed either

(i) A Single-Layer, Two-Block Design, with two blocks on a single radius R in the angular intervals 0 to θ_1 and θ_2 to θ_F;

(ii) A Single-Layer, Three-Block Design, with three blocks on a single radius, in the angular intervals 0 to θ_1, θ_2 to θ_3, and θ_4 to θ_F; or

(iii) A Two-Layer Design, with three blocks on a radius R_A in the angular intervals 0 to θ_1, θ_2 to θ_3, and θ_4 to θ_F, and two blocks on a radius R_B in the angular intervals 0 to ϕ_1 and ϕ_2 to ϕ_F.

In all cases the same current density (J_o amperes per meter of circumference) was assigned to all blocks. In the two-layer design the layer radii were taken to be in the ratio $R_B/R_A = 3.5/2.5$.

Analysis

In the material that follows the "harmonic order" is denoted by an index m that appears in terms proportional to $r^m \cos m\theta$ in a series development of the interior vector potential.

(i) Single-Layer, Two-Block Design:

Specification of the final angle θ_F permits one to seek values of θ_1 and θ_2 such that the harmonic components of order $m = 3$ and $m = 5$ each vanish.

The Fourier development of the current density in this configuration is

$$J_z(\theta) = \frac{4}{\pi} J_o \sum_{m=1,3,5,\ldots} \frac{\sin m\theta_1 - \sin m\theta_2 + \sin m\theta_F}{m} \text{ amp/m} ,$$

at the radius R, and the corresponding vector-potential component (MKS-A units) in the absence of image effects is

$$A_z = \frac{2\mu_o}{\pi} J_o \sum_{m=1,3,5,\ldots} \frac{\sin m\theta_1 - \sin m\theta_2 + \sin m\theta_F}{m^2} \begin{Bmatrix} r^m/R^{m-1} \\ \text{or} \\ R^{m+1}/r^m \end{Bmatrix} \cos m\theta$$

for $r < R$ or $r > R$, respectively. [The presence of image currents ($J = J_o R^2/R_{Fe}^2$, at a radius R_{Fe}^2/R), in a surrounding highly permeable iron cylinder of inner radius R_{Fe}, will act simply to increase each harmonic component of the interior field by the factor $1 + (R/R_{Fe})^{2m}$ in such a single-layer design.] The requisite conditions for the desired suppression of two harmonic components accordingly become, explicitly,

$$\sin m\theta_1 - \sin m\theta_2 + \sin m\theta_F = 0$$

for $m = 3$ and $m = 5$.

The two conditions written immediately above are sufficiently simple that for any assigned value of θ_F one can readily seek a solution (for θ_1 and θ_2) by a short sequence of successive trials -- aided, for example, by a simple VAX Program TRY35. Thus, for any θ_F, a trial value for θ_2 permits evaluation of $\sin 3\theta_1$ as $\sin 3\theta_2 - \sin 3\theta_F$ (and hence of θ_1 if $|\sin 3\theta_1| \leq 1$) so as to suppress the harmonic contribution for $m = 3$. With such provisional values for θ_2 and θ_1, an evaluation then can be made of the amount ("error") by which the desired condition for $m = 5$ is not satisfied. This error serves conveniently to guide the choice of an improved trial value for θ_2.

(ii) Single-Layer, Three-Block Design:

Specification of the final angle θ_F permits one to seek values of θ_1, θ_2, θ_3, and θ_4 such that the harmonic components of orders $m = 3,5,7$, and 9 each vanish. The requisite conditions are, explicitly,

$$\sin m\theta_1 - \sin m\theta_2 + \sin m\theta_3 - \sin m\theta_4 + \sin m\theta_F = 0$$

for $m = 3$, $m = 5$, $m = 7$, and $m = 9$. Solutions, for any assigned value of θ_F, are conveniently sought computationally by a program (such as that listed by V.O. Brady as SUPER.FOR;16) designed to employ the VAX version of the IMSL Routine ZSYSTM for solution of simultaneous nonlinear equations.

(iii) Two-Layer Design:

Specification of θ_1, θ_F, ϕ_1, and ϕ_F for the two-layer design permits one to seek values of θ_2, θ_3, θ_4, and ϕ_2 such that harmonic components of orders $m = 3,5,7,$ and 9 simultaneously vanish. The requisite conditions for this design then become (neglecting, for simplicity, the contributions from image fields):

$$\frac{\sin m\theta_1 - \sin m\theta_2 + \sin m\theta_3 - \sin m\theta_4 + \sin m\theta_F}{R_A^{m-1}} + \frac{\sin m\phi_1 - \sin m\phi_2 + \sin m\phi_F}{R_B^{m-1}} = 0$$

for $m = 3,5,7,$ and 9. Solutions are conveniently sought computationally by again employing the IMSL Routine ZSYSTM (as in the VAX program listed by V.O. Brady as SUPER.FOR;28).

Results

(i) Single-Layer, Two-Block Design:

With θ_F assigned successively various values $\geqslant 45°$, the corresponding values for θ_1 and θ_2 which simultaneously depress harmonic components of orders $m = 3$ and $m = 5$ are as shown in Table I and on Fig. 1. It is noted that for $\theta_F = 45°$ the widths of the individual blocks vanish ($\theta_1 \to 0$ and $\theta_2 \to \theta_F$). For values of θ_F in the neighborhood of 64° the requisite wedge thickness $\theta_2 - \theta_1$ is seen to pass through a minimum, and for a slightly larger value ($\theta_F \cong 67.275°$) the harmonic component of order $m = 7$ is found to vanish.

(ii) Single-Layer, Three-Block Design:

With θ_F assigned successively various values $\geqslant 60°$, the corresponding values of θ_1, θ_2, θ_3, and θ_4 which suppress harmonic components of orders $m = 3,5,7$, and 9 are as shown in Table II and on Fig. 2. It is noted that for $\theta_F = 60°$ the widths of the individual blocks vanish ($\theta_1 \to 0$, $\theta_2 \to \theta_3$, and $\theta_4 \to \theta_F$). For θ_F near 70° the requisite thickness $\theta_2 - \theta_1$ of the first wedge becomes quite small, and for a slightly larger value ($\theta_F \cong 71.830°$) the harmonic coefficient for $m = 11$ is found to vanish.

(iii) Two-Layer Design:

Many computational runs were made to examine two-layer configurations, with $R_B/R_A = 3.5/2.5$ (and image fields neglected), in which two wedges were present (per quadrant) to separate the three blocks on the inner layer and one additional wedge served to separate the two blocks on the outer layer. Specification of θ_1, θ_F, ϕ_1, and θ_F in these examples led to values of the remaining parameters such that harmonic components of orders $m = 3,5,7$, and 9 were simultaneously suppressed. It was noted early in the course of such work that in some instances distinctly different valid solutions can be obtained with respectively identical values of θ_1, θ_F, ϕ_1, and ϕ_F. Also, with other input values it was seen possible for the thickness of one block to become zero (e.g., $\phi_2 \to \phi_F$).

The results shown in Table III pertain to a sequence of runs that proved to be most useful in providing starting values for more realistic computations employing the program PARTIALKEYSTONE. The seventh entry in this table (for which $\theta_1 = 36°$, $\theta_F = 77°$, etc.) proved to be particularly helpful in leading to the final design (NC515, described in the body of this report), for which the use of three wedges on the inner layer finally proved to be attractive.

TABLE II.

APPROXIMATE VALUES (DEG.) TO SUPPRESS m=3, m=5, m=7, & m=9:

θ_F	θ_4	θ_3	θ_2	θ_1	Cumulative Width
80.	74.37686	59.46148	43.32350	37.66473	59.42585
79.	73.36668	59.12062	43.04977	37.49291	59.19708
78.	72.28562	58.71239	42.71853	37.28305	58.99129
77.	71.12834	58.22108	42.31315	37.02315	58.80274
76.	69.88562	57.62534	41.80860	36.69467	58.62579
75.	68.54341	56.89571	41.16565	36.26752	58.45417
74.	67.08167	55.99115	40.31948	35.68984	58.28984
73.	65.47367	54.85468	39.15634	34.86535	58.09002
72.	63.68797	53.41060	37.46237	33.59895	57.85921
71.82987	63.36444	53.12808	37.09552	33.31430	57.81229
71.	61.70327	51.57603	34.81266	31.46050	57.52510
70.5	60.64679	50.49925	32.89936	29.79949	57.25259
70.	59.58036	49.33168	30.45569	27.53661	56.83224
69.5	58.57237	48.11290	27.56639	24.63062	56.10476
69.	57.72983	46.89945	24.81364	21.49745	54.85343
68.5	57.11467	45.72954	22.91610	18.81733	53.01610
68.	56.69786	44.60886	21.92221	16.76125	50.75004
67.	56.28043	42.49523	21.49339	13.78764	45.50905
66.	56.24655	40.52118	22.01018	11.49026	39.75471
65.	56.48166	38.65368	22.93985	9.46080	33.69297
64.	56.91663	36.86333	24.09326	7.54976	27.40320
63.	57.50723	35.12482	25.39409	5.68785	20.91135
62.	58.22586	33.41591	26.81220	3.83285	14.21070
61.	59.05773	31.71539	28.34248	1.94992	7.26510
60.5	59.51472	30.86121	29.15352	0.98627	3.67924
60.	60.	30.	30.	0.	0.

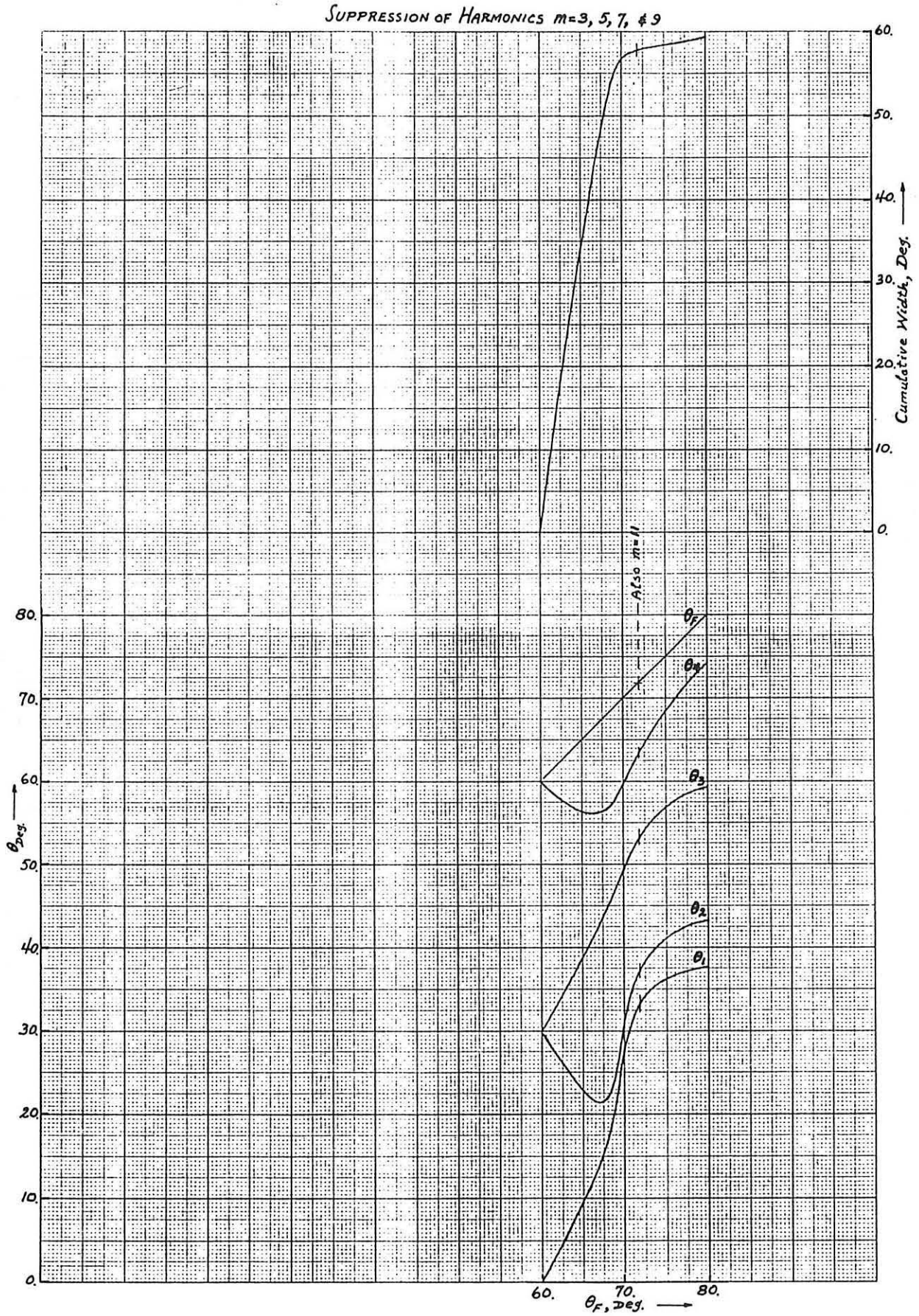
SUPPRESSION OF HARMONICS m=3, 5, 7, & 9
Cumulative Width, Deg.
0.
10.
20.
30.
40.
50.
60.
θ Deg.
80.
70.
60.
50.
40.
30.
20.
10.
0.
— Also m=11
θF
θ4
θ3
θ2
θ1
60.
70.
80.
θF, Deg.

Fig. 2

TABLE III

TWO-LAYER CONFIGURATION

Harmonics $m = 3, 5, 7, \& 9$ Suppressed

$R_A = 2.5$					$R_B = 3.5$		
θ_1	θ_2	θ_3	θ_4	θ_F	ϕ_1	ϕ_2	ϕ_F
44.	50.51983	61.85350	72.85777	78.	16.	37.65818	56.
44.	50.32118	61.31870	71.61606	77.	16.	37.79668	56.
42.6	48.71371	60.11161	70.73703	76.6	16.	36.42108	56.
40.	45.95695	59.34755	70.39956	77.	16.	32.12286	54.
38.	43.74771	59.02893	69.66214	77.	16.	27.72238	52.
37.	42.55702	59.02547	69.23933	77.	16.	24.85597	51.
36.	41.09967	59.23748	68.68347	77.	16.	20.74226	50.
36.	41.00593	58.17321	67.33777	76.	16.	22.76129	50.
36.	40.71630	56.94947	65.82612	75.	16.	24.73392	50.
35.	39.64990	56.78008	65.38204	75.	16.	21.80186	50.
34.	38.07399	56.76009	64.53497	75.	16.	17.05280	50.
34.	38.22230	56.72646	64.65161	75.	15.	16.61110	50.
34.	38.51367	56.65689	64.88266	75.	14.	16.75144	50.
36.	40.17453	55.47617	64.12840	74.	16.	26.99575	50.

Angles in degrees.

LAWRENCE BERKELEY LABORATORY
TECHNICAL INFORMATION DEPARTMENT
UNIVERSITY OF CALIFORNIA
BERKELEY, CALIFORNIA 94720